

Design and realization of a dual-wavelength low level light therapy for acne and face rejuvenation treatment

Napat Watjanatepin¹, Paiboon Kiatsookkanatorn², Chaoyant Boonmee¹, Sarayoot Thongkullaphat¹,
Tuanjai Archevapanich³, Patcharanan Sritanauthaikorn¹, Khanittha Wannakam¹

¹Solar Energy Research and Technology Transfer Center (SERTT), Rajamangala University of Technology Suvarnabhumi,
Nonthaburi, Thailand

²Department of Electrical Engineering, Rajamangala University of Technology Suvarnabhumi, Suphanburi, Thailand

³Department of Electronics and Communication Engineering, Rajamangala University of Technology Suvarnabhumi,
Nonthaburi, Thailand

Article Info

Article history:

Received Jan 22, 2022

Revised Sep 13, 2022

Accepted Sep 27, 2022

Keywords:

Acne treatment

Embedded system

Human machine interface

Low level light therapy

Skin rejuvenation

ABSTRACT

Low-level light therapy (LLLT) uses the light of wavelength between 400–700 nm to treat acne, reduce inflammation, stimulate collagen production, and rejuvenate the facial skin. This study designed and constructed a dual-wavelength LED LLLT device for the facial treatment. The light spectrum, power density, uniformity, stability, and safety of the device were analyzed. The proposed system consisted of an LED array with 415 and 633 nm wavelengths. Human machine interface with embedded system was used to control light intensity and treatment time. The phototherapy device is designed to be curvaceously sized to suit the face shape of Asian people. The results showed that the LLLT device emitted 633 ± 5 nm red and 415 ± 5 nm blue light with a linear adjustable light power density of $0-18.56$ mW/cm² and $0-3.70$ mW/cm², respectively. The spectrum distribution of the red and blue light was relatively constant over 30 minutes of operation. The uniformity and stability of red spectrum were about 89.9% and 95.08% and blue spectrum were 87.6% and 97.08%, respectively. The experimental face's temperature was below 31.5 °C. For the future study, the LED phototherapy device will be applied for clinical research in collaboration with dermatologists.

This is an open access article under the [CC BY-SA](https://creativecommons.org/licenses/by-sa/4.0/) license.



Corresponding Author:

Patcharanan Sritanauthaikorn

Solar Energy Research and Technology Transfer Center (SERTT),

Rajamangala University of Technology Suvarnabhumi

217 Suanyai, Muang, Nonthaburi, 11000, Thailand

Email: patcharanan.s@rmutsb.ac.th

1. INTRODUCTION

Rejuvenating facial skin is a beauty trend that meets the needs of the new generation. As a result, the beauty business in Thailand had a growth rate of more than 20% in the year 2019. They found that the new generation is most worried about their own face shape and also about acne and wrinkle problems on their face [1]. Acne problems such as acne vulgaris and inflammatory acne can be treated by using various antibiotics, which may have side effects. For example, if the same treatment is applied for a long time, it may cause drug resistance.

Phototherapy is another option that is used for both the treatment of Propionibacterium acne (P.acne) and the rejuvenation of the face because it is a safe method. Harmless light-emitting diodes (LEDs) are used as the light source because LEDs are semiconductor devices that emit light in a specific spectrum. In

narrow wavelengths, low-level light therapy (LLLT) or photodynamic therapy (PDT) is used for various skin treatments [2]. Each color of light has the potential to penetrate different layers of the skin. For instance, the blue LED (400-470 nm) has the potential to penetrate the dermis in the epidermis [3]. The red LED (630-670 nm) can penetrate and stimulate fibroblast that supports the re-production of the collagen in the dermis layer [4].

The blue light therapy is suitable for treating acne and killing bacteria on the skin layer. Sadowska *et al.* [5], Diogo *et al.* [6], and Opel *et al.* [7] stated a large number of documented reviews related to the use of blue LEDs phototherapy and they confirmed the conclusive findings that the light from blue LEDs (405-420 nm) was effective in mild to moderate inflammatory of the face treatment of the acne vulgaris and P.acne. In addition, some data [6], [7] indicated that light from the blue LEDs (400-470 nm) may also help treat the acne and P.acne.

Additionally, Barolet *et al.* [8] revealed that the 660 nm of red LED light was safe and effective in activating the new collagen under the skin and reducing facial wrinkles. This was consistent with Opel's finding [7] showed that the 630-700 nm red light has a beneficial effect on skin rejuvenation. This is consistent with the reports by Kim *et al.* [9] and Lee *et al.* [10], and the 640 nm red light combined with low-intensity IR light 830 nm was found to be effective in treating photo-aged skin [11]. Papageorgiou *et al.* [12] presented a combination of 415 nm blue light and 633 nm red light to improve the efficacy of acne treatment of 24 patients with mild to moderate facial acne. However, these clinical studies used phototherapy devices manufactured by relevant industries.

Some previous reports showed the design and construction of LED phototherapy systems. For example, the design and development of the multi-wavelength LED photo-rejuvenation system using LEDs as 455 nm blue, 661 nm red, and 828 nm far-red delivered high power density with a small beam aggregation [13]. Li *et al.* [14] presented the development multi-wavelength LLLT red LED of 633 and 660 nm, far-red LEDs of 810 and 940 nm. It was a portable device that emitted a 50 mm diameter of spot light. Liu *et al.* [15] developed a larger portable red-blue LED phototherapy system using 660 nm red and 450 nm blue LEDs. This system offered the lighting area of 50 cm × 25 cm with the light uniformity of 61 % and power density of 43 to 70 $\mu\text{W}/\text{cm}^2$. Nabizath *et al.* [16] reported the development of a phototherapy device with blue 450 nm combined with white LEDs with a size of approximately 56 cm x 48 cm including an image analysis system. Subsequently, Phan *et al.* [17] presented the development of LED light therapy device with power density control using red 633 nm, green 530 nm, and blue 470 nm LEDs. This device was used to treat the facial area to power density 40-60 mW/cm^2 .

This study, thus, focused on the LLLT phototherapy, because LLLT emits the light intensity that effects on the skin temperature lower than 40 °C that safe to the human skin [18]. The authors are not yet found a design and construct a 2-in-1 of LLLT device that is suitable for light therapy especially on the face and neck to treat acne and reduce wrinkles. The primary goal was to design and construct a LLLT dual-wavelength LED phototherapy device for the facial treatment. The secondary goal was to analysis of the light spectral, power density, power consumption, uniformity, stability, and safety of the prototype. This device could produce 633±5 nm red light and 415±5 nm blue light. It could adjustable the power density and estimate the dosing time of light therapy that can be calculated through the human friendly user interface.

2. PROTOTYPE DESIGN

2.1. Appearance design

The design goal is for the light therapy that the patient lies down during the treatment. The dimension of the equipment must be appropriate for the head and face size of Thai people according to the reference [19]. The average Thai head dimensions as: the length, width and depth are 19.22 cm, 16.83 cm, and 14.00 cm, respectively. The head and prototype dimensions were shown in Figure 1. The definitions of dimension could explain via Figure 1(a). The design of a LLLT dual-wavelength LED phototherapy was characterized and dimensioned via CAD drawing as shown in Figure 1(b). Letter A is the LED array module. B is a human machine interface module and C is shown the adjustable stand. Letter D is the lighting area of 0.11 m^2 (0.5 m×0.22 m).

2.2. Overall design scheme

The main components of the phototherapy system including the novel idea of 2-in-1 LED array were proposed in Figure 2. This system was composed of a LED array module, a micro-controller unit (MCU), a human machine interface module (HMI), and a pulse width modulation (PWM) LED driver module. The main power supply was a constant-voltage direct-current (DC) converter. It supplied to all main equipments of this system. The LED array module had a red and blue-LED array which controlled the power density of both lights independently with the MCU by using the PWM technique. The HMI was an important

device that received the control command and interacted with touch screen of a thin-film-transistor liquid-crystal display (TFT LCD). It was convenient and easy to access. All components were mounted in an elegant chassis (Figure 1) which molded in acrylonitrile butadiene styrene (ABS) plastic and constructed by a 3-dimension (3D) printer.

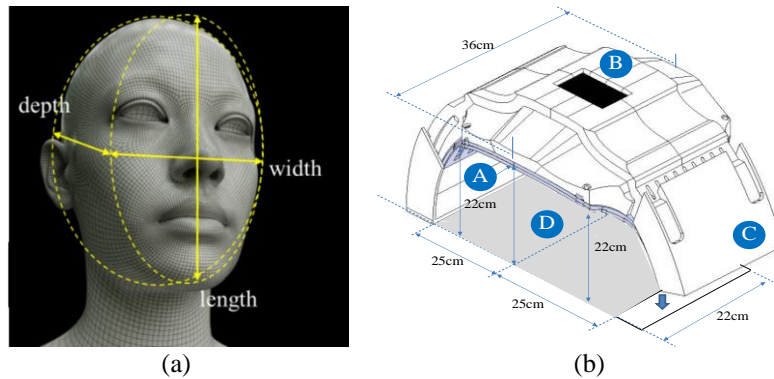


Figure 1. Head and prototype dimension (a) Model of Thai human head and (b) Drawing of a prototype of LLLT dual-wavelength LED phototherapy

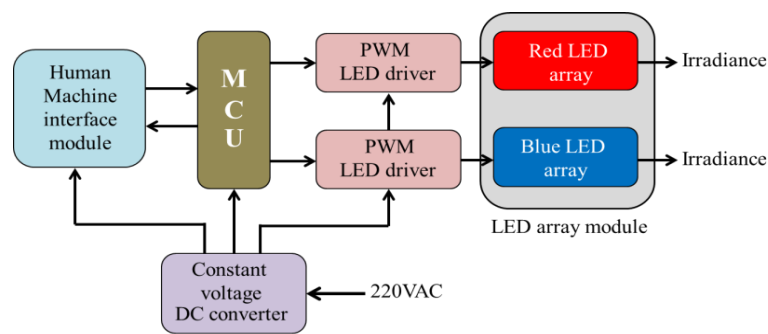


Figure 2. An overall design of the LLLT dual-wavelength LED phototherapy device

2.2.1. 2-in-1 LED array module

According to the previous literature, the phototherapy means bio activation or bio inhibition based on the optical properties of tissues and the dosing parameters of the light [20]. These parameters should include at least the type of light source, wavelength, optical power, energy, radiation exposure (J/cm^2) irradiation or power density (W/m or mW/cm^2) and the mode of use of the device (wearable, portable or distance). In this paper, the design goal was set as a power density of red light of $10mW/cm^2$ and blue light of $20mW/cm^2$, which was a light intensity suitable for LLLT phototherapy [5], [6], [17], [21]. The authors focused on selecting the LED spectrum to meet the research objectives. These LEDs were purchased domestically, with this limitation; the authors had to choose red and blue LEDs with different specifications. In other words, the 633 nm red LED is the 5050 surface-mount device (SMD) mounted thin film strip and the 415 nm blue LED is a bread type high power LED as in Figure 3. Dimension of each letters of LED installation map were $A=22$ cm, $C=3$ cm, $D=6$ cm, $E=3.5$ cm, $F=60$ cm, $G=30$ cm, and $H=1.5$ cm. LEDs area were $LA_{IB}=6\text{ cm}\times3.25\text{ cm}=19.5\text{ cm}^2$ and $LA_{IR}=5.75\text{ cm}\times3\text{ cm}=17.25\text{ cm}^2$. Luminaire area was cover with one blue LED and one unit (3 LEDs) of red LED. The total lighting area was around $1,590\text{ cm}^2$ (0.159 m^2). The characteristics of blue and red LEDs were shown in Table 1. The blue and red LEDs were simulated to determine photosynthetic photon flux density (PPFD) and converted to power density (PD_{ILED} in W/m^2) by (1) and (2). The online simulating tool was “horticulture lighting system calculation” provided by OSRAM Opto semiconductor. The total electric power (Pe_{TOTAL}) and total power density (PD_{TOTAL}) of the LED light source were shown in Table 1. As shown in (1) and (2) were created by the experiment in our laboratory, to find out the relationship between PPFD versus power density of 415 ± 5 nm blue and 633 ± 5 nm red (the details are not shown in this paper). From (1) and (2), the PD_B and PD_R were the power density (W/m^2) of 415 ± 5 nm blue and 633 ± 5 nm red LEDs, respectively.

$$PPFD_B = 0.59260 PD_B + 0.45660 \tag{1}$$

$$PPFD_R = 0.50706 PD_R - 2.86420 \tag{2}$$

where LA: luminaire area (cm²) per one LED (as shown in Figure 3), LT: total luminaire area (cm²), Pe=V_f×I_f: electric power input of a LED (V_f is forward voltage, I_f is forward current), Pe_{TOTAL}: electric power consumption of LED array, PD_{TOTAL}: total power density of LED array at distance 15 cm from the light source. ^A PPFD in μmol m⁻²s⁻¹ by simulation, ^B PD_B: power density from one blue LED by using equation (1), ^C PD_R: power density from one unit of red LED by (2).

From Table 1, the total number of the blue LEDs was 84. There was combination of 4 series and 21 branches in parallel. The total power consumption of the blue LED was estimated around 84 W. The red LED circuit was combination of 3 LEDs in series and 132 branches in parallel. Total number was 396. In practical, to symmetrize red LEDs number, the proposed system used 3 series and 144 branches so it was 432 in total. The estimated total power consumption of red LED array was around 95.04 W.

The pattern and installation location of both LEDs types were shown in Figure 3. The LED array module was designed with two light source areas; the central part was an oval that covered the entire face. The lateral portion rectangular covered the side of the head and ears. The goal was to ensure that all facial surfaces received light therapy at the same intensity as possible. The uniformity test results were listed in the results and discussion section.

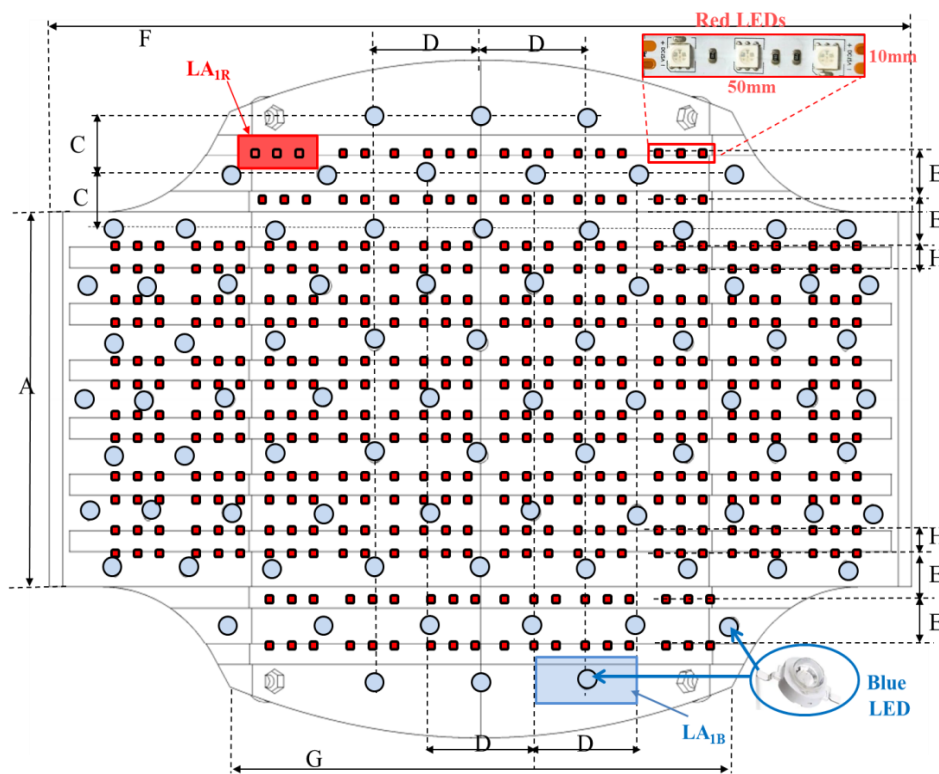


Figure 3. The LED installation map of red and blue LEDs of 2-in-1 LED array module

Table 1. Simulated and calculated results of PPFD, Pe_{TOTAL}, and PD_{TOTAL} of the light source

LED	LA (cm ²)	LT (cm ²)	PPFD ^A (μmol m ⁻² s ⁻¹)	PD _{I,LED} (W/m ²)	Number of LED	Pe _{TOTAL} (W)	PD _{TOTAL} (mW/cm ²)
B(439 – 461nm), V _f =3.2V, I _f =0.3A, Pe _B =1W	19.50	1590	2.0	2.60 ^B	84	84	21.8
R(612 – 630nm), V _f =6.3V, I _f =60mA, Pe _R =0.72W	17.25	1590	1.0	0.76 ^C	396	95.04	10.0

2.2.2. Micro-controller unit

The proposed system used a micro-controller ESP-WROOM-32 as a processing device. Main reason was small size, light weight and low power consumption. A micro-controller ESP32-D0WDQ6 was a CPU and CPU clock frequency was wide from 80 MHz to 240 MHz. The ESP-WROOM-32 could directly interface to the PWM driver module. It was suitable for driving the LED driver module. It could also be connected via Wi-Fi and Bluetooth well, so smart control can be extended in the future. It was fitted for small area inside the proposed prototype. The MCU was programmed to allow user to modify controlled parameters such as LED's color, duty cycle, and time for therapeutic applications.

2.2.3. Human machine interface module

In general, the HMI is widely used in industrial sectors involved in process control of the plant by using the programmable logic controller [22]. Nowadays, the HMI included a graphical user interface (GUI) could apply to smart home, smart agriculture, and smart equipment [23], [24]. The authors' intention was to design for users' friendly access with this device as Figure 4. Interactive display was shown in Figure 4(a). Authors chose a large TFT touch screen of 4.3-inch Nextion intelligent series HMI touch display as the main device to link the machine and the user as Figure 4 (b). This device had 32MB flash memory and 8kB RAM with real-time clock. It could communicate via the UART port that connected to the author's choice of MCU as well. The HMI module consisted of a resistive touch panel size of 105.50×67.20 mm (model NX4827K043-001R) and a control board mounted smoothly behind the touch panel. The assembled dimension was 120×72×6.4 mm. The human machine interface module would support data communication, data storage, and connection with other devices. The HMI module was at letter B in Figure 4(c).

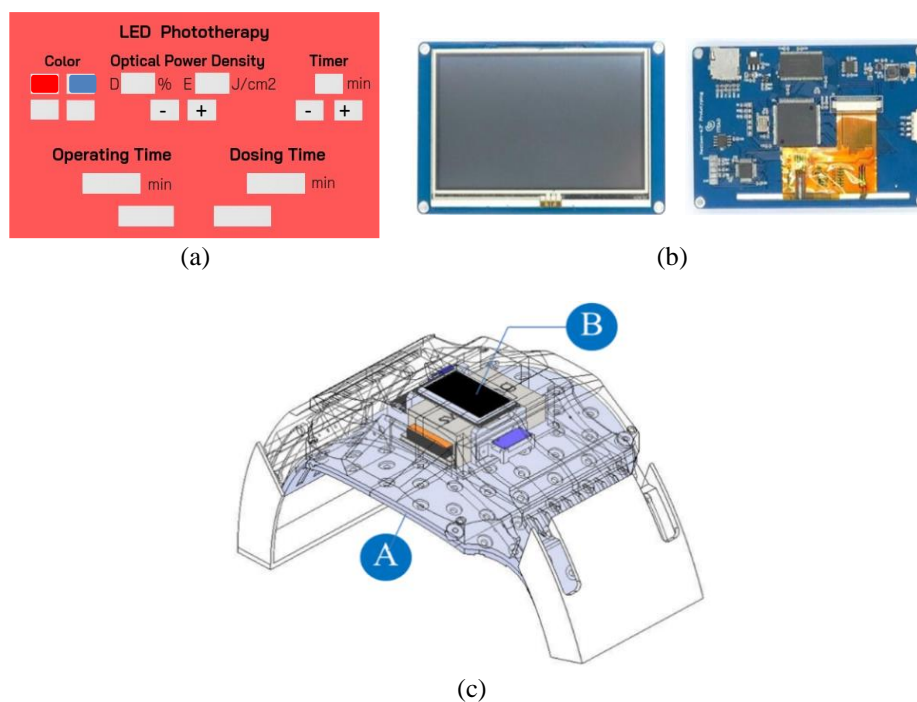


Figure 4. HMI module, (a) A graphical user interface on screen of a HMI module, (b) The front and back of the HMI model NX4827K043-001R, and (c) Novel design of 2-in-1 LED module. Letter A was LED module and B was the HMI module

2.2.4. LED driver module

The red LED array with 432 LEDs connected to the 12V 100 W power supply. The 84 blue LEDs with 415 nm were connected to the same power supply. LED driver circuits of blue and red LED array were displayed in Figure 5. Two separated drivers were designed by using 2 channel power MOSFET (IRF3205) module including opto-isolator input as shown in Figure 5(a) for blue LEDs and Figure 5(b) for red LEDs. The power density of each LED array was controlled by user through a HMI module. The percentage of duty cycle could adjust from 0 to 100% on the touch screen of HMI as shown in Figure 4(a). The input of each

driver received the PWM signal from MCU. The PWM controlled the duty cycle of power MOSFET, it drove the power density of the LED array module.

2.3. Software design

2.3.1. Human machine interface

The controller, display, and interface of HMI program was written by Nextion editor together with hardware compatible to support efficient HMI development. The Nextion Editor is a unique program called an “integrated development environment”. It means that there are all tools necessary to integrate into one screen. It does not need to open and close a lot of command windows. It is an easy-to-use and time-saving tool for developing GUI for HMI. The HMI system has a processor that supports the single-tasking, multi-tasking, and display for GUI. The developed GUI was able to select the color of the LED, adjust the level of power density, set the phototherapy time, and display the total treatment time. The GUI via HMI module was shown in Figure 4(a). The touch screen of the HMI module could receive and monitor all commands.

2.3.2. Software flowchart

The ESP-WROOM-32 used Arduino C++ to develop the software program. The operation flow chart was shown in Figure 6. The program started by initializing variables such as color of LED, time, and duty cycle control. Next, user had to input commands such as selecting the color of the LED, duty cycle and a treatment time. The program calculated the dosing time and displayed other parameters on the screen of HMI module. When the start button was pressed, the phototherapy device would be turned on until the operating time equal to the setting time. The device, then, would be turned off. However, user could press the stop button during treatment for turning off device any time.

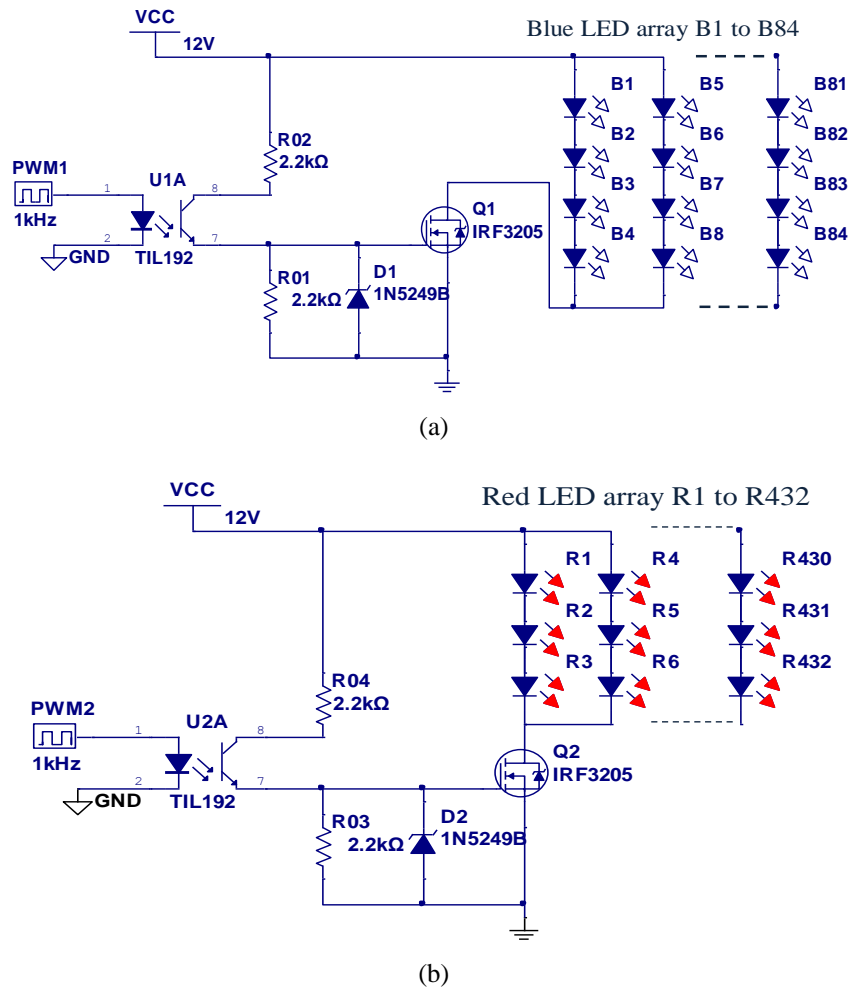


Figure 5. LED driver circuits, (a) driver of a blue LED array and (b) driver of a red LED array

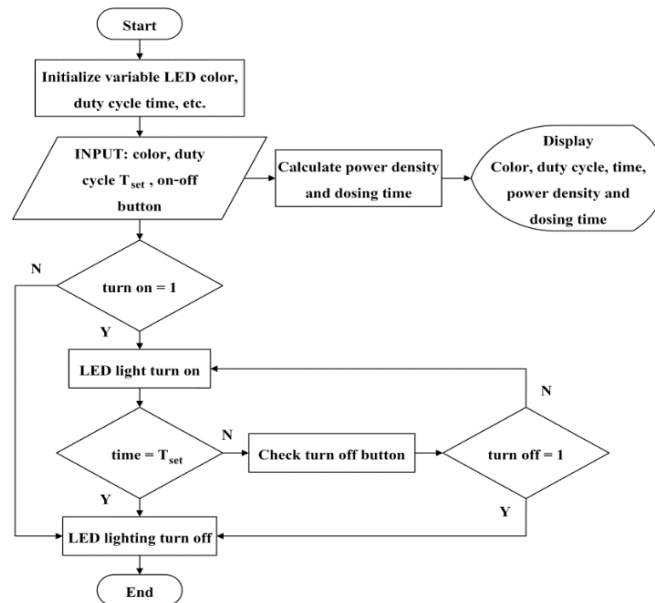


Figure 6. Software flowchart of control and operation of a LLLT dual-wavelength LED phototherapy device

3. RESULTS AND DISCUSSION

3.1. LED spectral analysis

A spectroradiometer (Lighting Passport™) was used to measure the spectral distribution of the LED array at the center of the test area. The control parameters are: the duty cycle was equal to 100%, the light was blue, and the operating time was 30 min. Then, the start button was pressed on the touch screen. The measurement results were recorded at 2 and 30 minutes after the LED phototherapy was turned on and the analyzed spectrum was done with a software application called “Spectrum genius Essene”. The red light was set up as the same method of the blue light. The measurement results showed as spectral irradiance in Figure 7 that the wavelength at the center of the blue light spectrum was 418 nm and 420 nm, respectively. The red peak spectrum was 628 nm and 631 nm. The full width at half maximum (FWHM) of blue and red light was analyzed as 28 nm and 24 nm, respectively, as shown in Figure 7(a) and (b). The results of the analysis showed that the LED spectral emission was consistent with the goals of the design. There were red of 633±5 nm and blue of 415±5 nm. Typically, an LED was turned on continuously for a long time, its temperature at p-n junction gradually increased. This higher temperature resulted in decreasing irradiance and slightly shifting the peak of the light’s wavelength. When good heat dissipation was provided to the LEDs, this change was only minimal as shown in Figure 7(c).

3.2. Adjustment of power density

A pyranometer (CMP3, Kipp, and Zonen) was used to measure the light power density in W/m² and it then converted to mW/cm² as spectral irradiance. The measurement results were shown in Figure 8. The pyranometer was placed at 15 cm away from the light source at the center of the lighting area as Figure 8(a) and adjusted the duty cycle from 0 to 100% (10% interval). These measurement results were recorded by a SOLRAD data logger. The light power density with duty cycle and total power consumption with power density of blue light showed on Figures 8(b) and (c), respectively. Figures 8(d) and (e) were the results of red light. At Figures 8(b) and (d), the light power density of the blue and red LEDs was linearly proportional to the duty cycle of the PWM signal. The results showed that the power density of blue light from the developed phototherapy can be adjusted from 0-18.56 mW/cm², which was closed to the target PD_{TOTAL} of 20 mW/cm². The power density of red light was adjustable from 0-3.70 mW/cm², which was quite less than the target value. The probable main cause was due to the ability of an LED to convert input power to optical power output, namely wall plug efficiency or WPE. The red LED used in this study was lower WPE than that of red (612-630 nm) that showed in Table 1. It could prove by calculating WPE from the experimental results; the WPE was about 5.98 %.

$$(WPE = \frac{P_{optic}}{P_e} \times 100\% = \frac{4.07W}{68.04W} \times 100\% = 5.98\%, P_{optic} = \frac{37W}{m^2} \times 0.11m^2 = 4.07 W)$$

Whereas WPE obtained from simulation results was about 20% ($WPE = \frac{0.2W}{1W} \times 100\%$). The experimental results were also inconsistent with the simulation result and the results of a study by Zhang *et al.* [25] reported that the WPE of 608 nm red LED at 0.8 A/cm^2 was about 24%. The maximum power consumption of blue and red LEDs array were about 71.63 W and 68.04 W of 18.56 mW/cm^2 and 3.7 mW/cm^2 , respectively.

The control of the LED power density through an LED driver using PWM switching techniques in combination with a digital platform was ideal because of its precision and linearity. Many previous researchers had used this method with a microcontroller. The processor was as STM-32, Arduino, and AVR [13]-[16], [21], [26]. Figure 8(c) showed a linear relationship between total power consumption and power density of blue LED light, the maximum power of 71.64 W gave a PD_{TOTAL} value of 18.56 mW/cm^2 . For a $633 \pm 5 \text{ nm}$ red LED, the relationship between P_{TOTAL} versus PD_{TOTAL} was shown in Figure 8(e) as linear direct proportion. The maximum power consumption was 68.04 W. The PD_{TOTAL} of red light was 3.70 mW/cm^2 . This was reasonable because the photon energy of the light of $415 \pm 5 \text{ nm}$ wavelengths was proportionally greater than that of the $633 \pm 5 \text{ nm}$ wavelengths, which followed an equation $E = \frac{hc}{\lambda}$ as described in Phan *et al.* [17]. Where λ was wavelength, h was the plank's constant (6.626×10^{-34}). c was light velocity ($3 \times 10^8 \text{ ms}^{-1}$).

The LLLT phototherapy device in this paper was designed with a distance of 15 cm between the patient's face and the light source in order to provide a proper distance and reduce the heat effect on the skin. The research of Mahdi and Jawad [27] that used laser beam revealed that the distance is more than 400 nm, temperature is undetected in tissue.

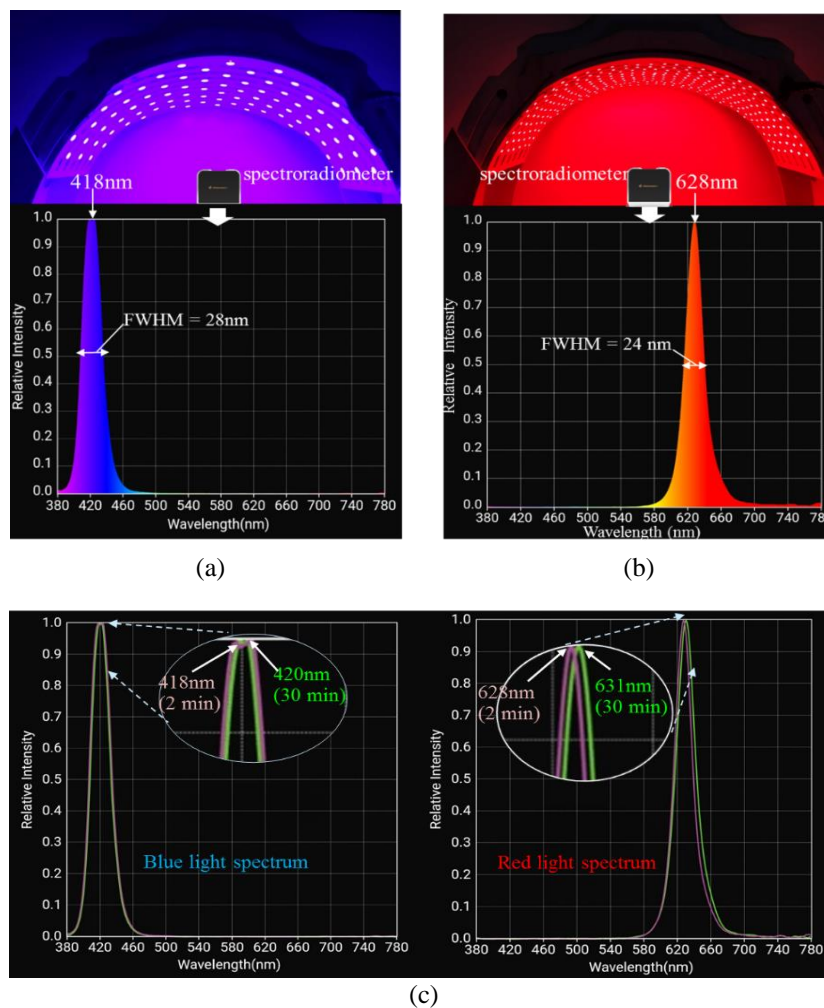


Figure 7. Spectral irradiance, (a) measurement result of spectral irradiance of blue LEDs, (b) measurement result of red LEDs spectral distribution, and (c) comparative spectral irradiance of blue and red LEDs over 2 min and 30 min of operation

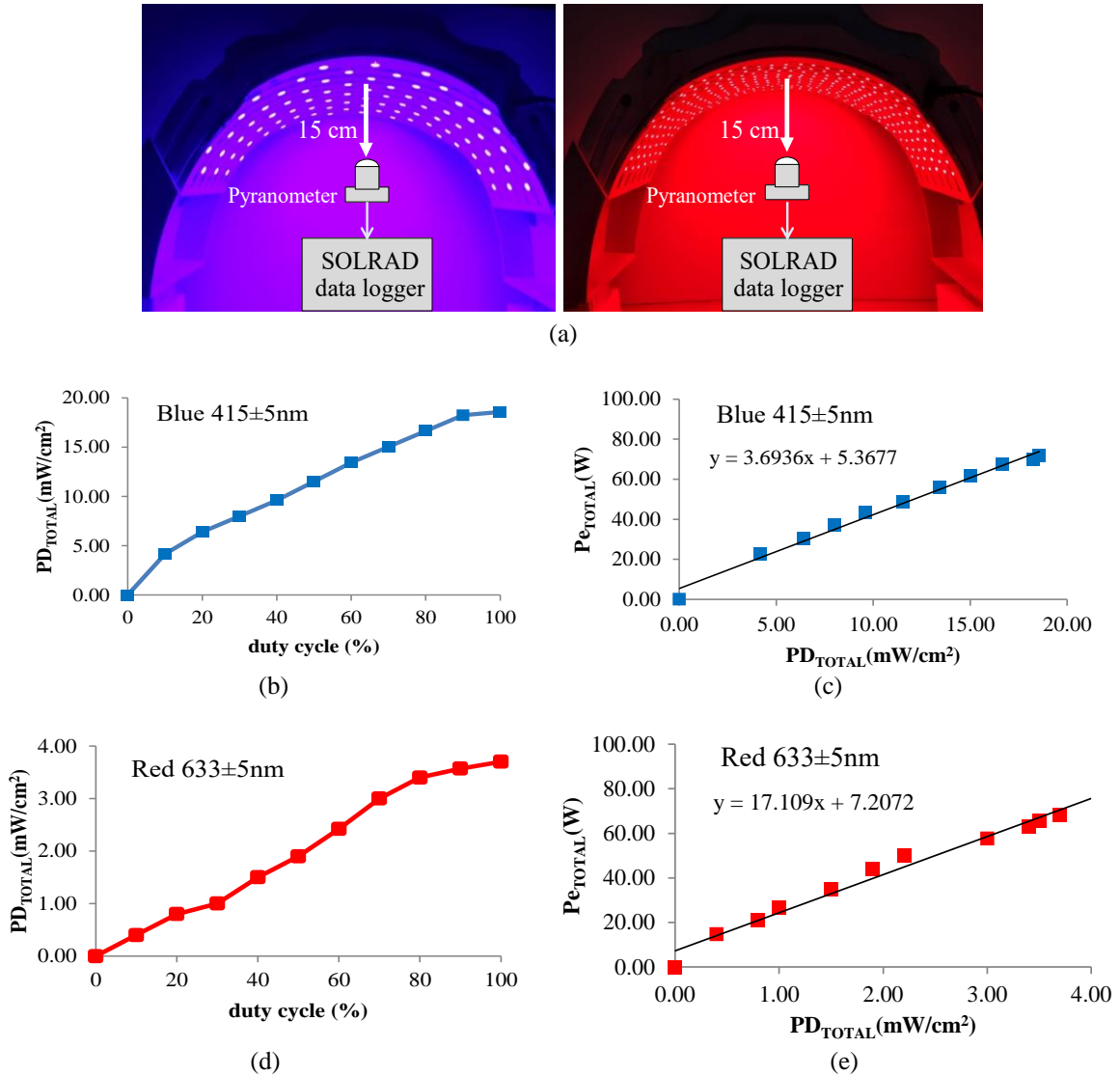


Figure 8. Measurement results, (a) measurement diagram of light power density, (b) the linear relationship of PD_{TOTAL} versus duty cycle, (c) a P_{eTOTAL} versus PD_{TOTAL} of the blue LED, (d) and (e) indicated the linear relationship of PD_{TOTAL} versus duty cycle and the P_{eTOTAL} versus PD_{TOTAL} of the red LEDs light

3.3. Light uniformity analysis

Light power density was measured in our laboratory with a Quantum/PAR Meter with external sensor (3415FXSE/Spectrum technology, Inc.), wavelength range 400–700 nm, 0–1999 μmol m⁻²s⁻¹, ±5%. The meter has a small external sensor. While measuring light power density on the face models, it is more convenient and faster than using a pyrometer like the previous topic. The measured result of the optical power density did not need to be converted to W/m² or mW/cm² because determination of the uniformity of light was calculated from the maximum and minimum values of light energy per area as (3).

$$Light\ uniformity = \left[1 - \frac{E_{MAX} - E_{MIN}}{E_{MAX} + E_{MIN}} \right] \times 100\% \tag{3}$$

where E_{MAX} is maximum irradiance and E_{MIN} is minimum irradiance.

It was adapted from the equation non-uniformity of irradiance [28], [29]. A rigid form face model was created with appearance and dimensions consistent with the simulated face from Figure 1(a) and divided the phototherapy-treated face into 9 sections, A1–C3, as shown in Figure 9. The form face model was placed on a flat surface of the light therapy device at table center, 15 cm away from the light source. The LLLT phototherapy device was switched on and selected on the red light at 100% duty cycle. After 2 min., the light

will be stable, and then the light power density was measured one place at a time until complete. Later, device was turned off, it had to wait for the temperature of the device to be equal to room temperature, and then the measurement was repeated for 3 cycles and averaged each light position. The same experiment was done for blue light. The results showed that the light uniformity of red and blue light was quite similar, 89.9% and 87.6%, respectively, as shown in Figure 9. The results of this system were consistent with the LED phototherapy device of Li *et al.* [14] and had significantly better light uniformity than the LED phototherapy system by Liu *et al.* [15]. The uniformity of light was related to the layout of the LED luminaire, the distance of the light source, and the temperature of the LEDs [15], [28]. Light uniformity measured above 80% was a relatively high figure indicating that symmetrical LED light source design and installation location were appropriate. The phototherapy participants received light of equal power density. It resulted in a good treatment effect and ensured that the proposed LLLT phototherapy device was suitable for acne treatment and rejuvenating the face's skin of the patient. However, for therapy, it may be necessary to prevent side-effects that may occur on the eye and the lips areas. The authors recommended using blackout goggles to prevent and reduce the effects of light on the eye area [17]. The treatment light of the proposed LLLT device provided the very good light-uniformity on the face model. After 30-minute continuous operation, the spectral of the red light and blue light remained in the range of $633 \pm 5\text{nm}$ and $415 \pm 5\text{nm}$, respectively. The results of this proposed LLLT tend to be supported an effective treatment of acne, wrinkle and face rejuvenation [4], [8], [15].

3.4. Stability analysis

Light stability is analyzed by measuring light power density change of light sources, how they are stable or how much the density has changed. In this study, red and blue light stability was measured and analyzed. The conditions of this LED phototherapy device were duty cycle control of 100% and continuous operation of 30 minutes with warm-up time of 2 minutes. By using the same measuring instrument as section 3.2, measurement results were shown in Figure 10. Red and blue dot-line showed the power density versus time. The maximum and minimum measurement results were then analyzed for light stability with (4) such the equation improved from temporal equations instability of irradiance of IEC 60904-9 edition 2 [28].

$$\text{Light stability} = \left[1 - \frac{E_{MAX} - E_{MIN}}{E_{MAX} + E_{MIN}} \right] \times 100\% \quad (4)$$

According to the results, E_{MAX} and E_{MIN} were about 17.6 W/m^2 and 16.6 W/m^2 for blue light and E_{MAX} and E_{MIN} were 3.6 W/m^2 and 3.3 W/m^2 for red light. The stability of blue light and red light was 97.08% and 95.08%, respectively. From the experiment, the results were concluded that the proposed LLLT-LED phototherapy device offered very good light stability. This indicated that the heat control of the LED was appropriate, resulting in the power density from both LEDs being changed by less than 5%. It is because the cooling system of the LED made the temperature not too high. Therefore, the power density of the light was kept relatively constant throughout the working period of the LED phototherapy device [28], [29].

3.5. Safety analysis

The LLLT phototherapy device is a device that emits low intensity light for therapeutic purposes. The emitted light must not cause the temperature of the exposure region over $40\text{ }^\circ\text{C}$. The property of LLLT should be under this temperature. The intensity of the photon flux increases the reactivity in the cells but it does not damage those cells [18]. In this study, the authors measured the surface temperature of the treated patient comparing to the LED's temperature and room temperature. Using a digital thermometer with data logger, the temperature was continuously recorded throughout the 30-minute operation of the device. Figure 11 revealed the test area and the temperature. The temperature probe was stucked on the patient face as Figure 11(a). The results showed that the maximum surface temperature of the blue and red light treated recipients were $31\text{ }^\circ\text{C}$ and $31.5\text{ }^\circ\text{C}$, respectively. The highest temperatures of the blue and the red LEDs were $36.5\text{ }^\circ\text{C}$ and $35.5\text{ }^\circ\text{C}$, respectively, when the average room temperature was $25\text{ }^\circ\text{C}$ as shown in Figure 11(b) and (c). These results were consistent with the use of a wearable flexible phototherapy device by Liu *et al.* [26] to produce a skin temperature of $32\text{ }^\circ\text{C}$ after 10 min of continuous operation. The proposed LLLT phototherapy was safer than the multi-wavelength high irradiance phototherapy device of Li *et al.* [14] with a skin temperature of $42.5\text{ }^\circ\text{C}$ at 30 min. Summary, the proposed LLLT dual-wavelength LED phototherapy was safe. The temperature at the surface of the treatment recipient was not higher than $31.5\text{ }^\circ\text{C}$ over 30 minutes which does not adversely affect or destroy facial skin cells [18].

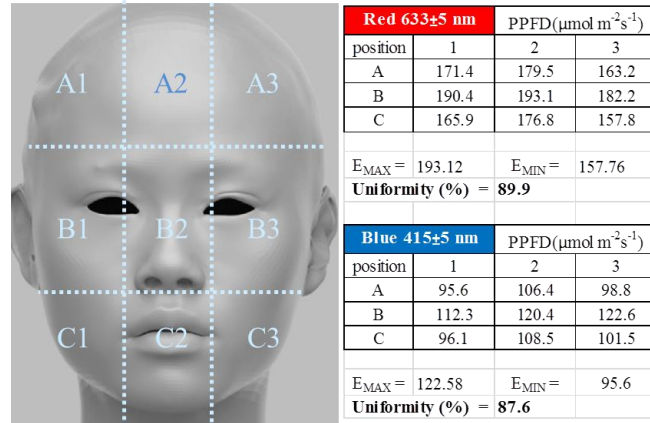


Figure 9. Measurement of light power density and analysis the light uniformity on the face model

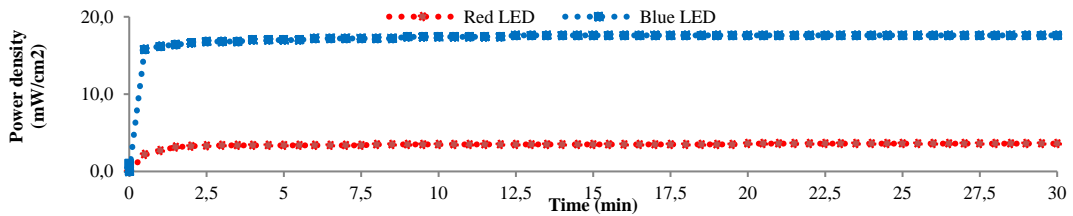
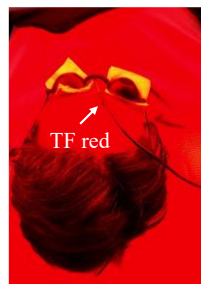
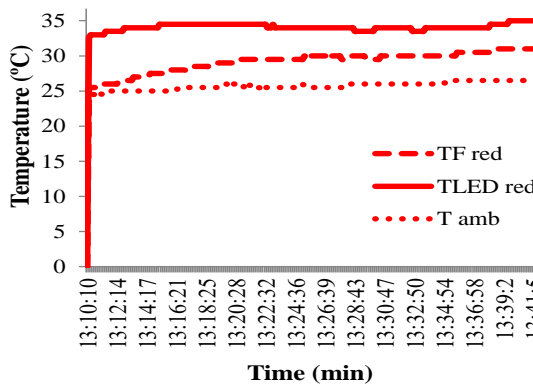


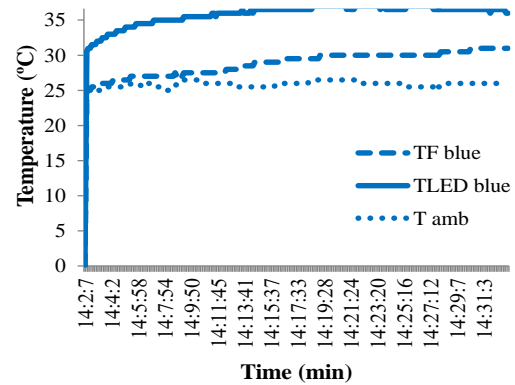
Figure 10. Measurement results of power density of the blue and red light



(a)



(b)



(c)

Figure 11. The safety analysis; (a) temperature probe on the patient's face under red light therapy, (b) measurement results of temperature from red LED, and (c) blue LED; TF red: temperature on the face from red light, TLED red: temperature of red LED, T amb: ambient temperature, TF blue: temperature on the face from blue light, TLED blue: temperature of blue LED

4. CONCLUSION

In conclusion, the proposed LED phototherapy device was presented. The 2-in-1 light therapy was available; the red light of 633 ± 5 nm and blue light of 415 ± 5 nm. The HMI device with a 4.7-inch touch screen was applied for more convenient and user-friendly operation. The HMI device was compatible with the microcontroller. It could be seamlessly set to completely control the various parameters in therapeutic treatment. The microcontroller ESP-WROOM-32 was used to control light intensity and time. The optical power density was adjusted by PWM technique for the blue light and the red light. They were $0\text{--}18.56$ mW/cm^2 and $0\text{--}3.70$ mW/cm^2 , respectively. The blue and red-light spectra changed a bit insignificantly when the device had been operated continuously for 30 minutes. Light uniformity and light stability caused by blue and red light on the test area were higher than 95% and 87%, respectively. This device was safe for light therapy applications. Safety results confirmed that the temperature at the surface of the treatment recipient was around 31.5 °C over 30 minute period of operation. The software tool “horticulture lighting system calculation” was an application for designing the artificial lighting for the modern plant cultivation. It could be used instead of making a light source like the phototherapy device. If this LLLT prototype is interested by an entrepreneur, it can be scaled up for commercial use. This will make this technology cheaper, reduce imports from abroad, and easier access for patients’ treatment. It is safe to compare to antibiotic treatment. The limitation of this study is the restrictive duration of this research project. This made the author unable to supply the red LED of 633 ± 5 nm with high power type from abroad in time. Therefore, it was necessary to choose an SMD 5050 LED strip 633 ± 5 nm that was purchased locally as a replacement, resulting in LEDs with lower than expected energy conversion efficiency. This resulted in the maximum power density of the red LED not meeting the target. The future research plans, the authors hope to continue applying our LED phototherapy device for clinical research in collaboration with dermatologists at Phra-nang-khao Hospital, Nonthaburi, Thailand.

ACKNOWLEDGEMENTS

Authors would like to thank Rajamangala University of Technology Suvarnabhumi for a partial funding support in 2021.





REFERENCES

- [1] J. Survey, “Beauty Trend 2020 (in Thai).” <http://siamrath.co.th/n/163962> (accessed Mar. 07, 2022).
- [2] A. Huang, J. Nguyen, D. Ho, and J. Jagdeo, “Light emitting diode phototherapy for skin aging,” *Journal of Drugs in Dermatology*, vol. 19, no. 4, pp. 359–364, Apr. 2020, doi: 10.36849/JDD.2020.4711.
- [3] D. P. Friedmann, M. P. Goldman, S. G. Fabi, and I. Guiha, “The effect of multiple sequential light sources to activate aminolevulinic acid in the treatment of actinic keratoses: A retrospective study,” *Journal of Clinical and Aesthetic Dermatology*, vol. 7, no. 9, pp. 20–25, 2014.
- [4] P. Avci, A. Gupta, M. Sadasivam, D. Vecchio, Z. Pam, N. Pam, and M. R. Hamblin, “Low-level laser (light) therapy (LLLT) in skin: stimulating, healing, restoring,” *Seminars in cutaneous medicine and surgery*, vol. 32, no. 1, pp. 41–52, 2013, [Online]. Available: <https://pubmed.ncbi.nlm.nih.gov/24049929/>.
- [5] M. Sadowska, J. Narbutt, and A. Lesiak, “Blue light in dermatology,” *Life*, vol. 11, no. 7, 2021, doi: 10.3390/life11070670.
- [6] M. L. G. Diogo *et al.*, “Effect of blue light on acne vulgaris: A systematic review,” *Sensors*, vol. 21, no. 20, 2021, doi: 10.3390/s21206943.
- [7] D. R. Opel *et al.*, “Light-emitting diodes: A brief review and clinical experience,” *Journal of Clinical and Aesthetic Dermatology*, vol. 8, no. 6, pp. 36–44, 2015.
- [8] D. Barolet, C. J. Roberge, F. A. Auger, A. Boucher, and L. Germain, “Regulation of skin collagen metabolism in vitro using a pulsed 660nm LED light source: clinical correlation with a single-blinded study,” *Journal of Investigative Dermatology*, vol. 129, no. 12, pp. 2751–2759, Dec. 2009, doi: 10.1038/jid.2009.186.
- [9] S. K. Kim, H. R. You, S. H. Kim, S. J. Yun, S. C. Lee, and J. B. Lee, “Skin photorejuvenation effects of light-emitting diodes (LEDs): a comparative study of yellow and red LEDs in vitro and in vivo,” *Clinical and Experimental Dermatology*, vol. 41, no. 7, pp. 798–805, Oct. 2016, doi: 10.1111/ced.12902.
- [10] Y. I. Lee *et al.*, “The use of a light-emitting diode device for neck rejuvenation and its safety on thyroid glands,” *Journal of Clinical Medicine*, vol. 10, no. 8, 2021, doi: 10.3390/jcm10081774.
- [11] W. Li, I. Seo, B. Kim, A. Fassih, M. D. Southall, and R. Parsa, “Low-level red plus near infrared lights combination induces expressions of collagen and elastin in human skin in vitro,” *International Journal of Cosmetic Science*, vol. 43, no. 3, pp. 311–320, Jun. 2021, doi: 10.1111/ics.12698.
- [12] P. Papageorgiou, A. Katsambas, and A. Chu, “Phototherapy with blue (415 nm) and red (660 nm) light in the treatment of acne vulgaris,” *British Journal of Dermatology*, vol. 142, no. 5, pp. 973–978, May 2000, doi: 10.1046/j.1365-2133.2000.03481.x.
- [13] J. Chen, L. Guo, J. Wang, Y. Chen, Q. Zheng, and D. Xiong, “Design of a multi-wavelength LED photo-rejuvenating system,” in *2018 15th China International Forum on Solid State Lighting: International Forum on Wide Bandgap Semiconductors China (SSLChina: IFWS)*, Oct. 2018, pp. 1–4, doi: 10.1109/IFWS.2018.8587317.
- [14] W. Li, Z. Jin, J. Liu, L. Guo, H. Wang, and D. Xiong, “Design of a multi - wavelength high irradiance LED phototherapy system for LLLT,” in *2019 16th China International Forum on Solid State Lighting & 2019 International Forum on Wide Bandgap Semiconductors China (SSLChina: IFWS)*, Nov. 2019, pp. 175–179, doi: 10.1109/SSLChinaIFWS49075.2019.9019817.
- [15] K. Liu, L. He, and Y. Sun, “Development of a portable red-blue light emitting diode phototherapy system,” in *Proceedings - 2017 Chinese Automation Congress, CAC 2017*, Oct. 2017, vol. 2017-January, pp. 2077–2080, doi: 10.1109/CAC.2017.8243113.





- [16] M. A. Nabizath, S. A. Soumya, V. Boomitha, C. Meena, and P. Sridharan, "New design for phototherapy device and skin colour analysis," in *2017 IEEE International Conference on Smart Technologies and Management for Computing, Communication, Controls, Energy and Materials (ICSTM)*, Aug. 2017, pp. 253–257, doi: 10.1109/ICSTM.2017.8089163.
- [17] D. T. Phan *et al.*, "Development of a LED light therapy device with power density control using a Fuzzy logic controller," *Medical Engineering & Physics*, vol. 86, pp. 71–77, Dec. 2020, doi: 10.1016/j.medengphy.2020.09.008.
- [18] R. G. Calderhead and Y. Tanaka, "Photobiological basics and clinical indications of phototherapy for skin rejuvenation," in *Photomedicine - Advances in Clinical Practice*, InTech, 2017.
- [19] P. Mahakkanukrauh *et al.*, "Cranio-metric study for sex determination in a Thai population," *Anatomy & Cell Biology*, vol. 48, no. 4, p. 275, 2015, doi: 10.5115/acb.2015.48.4.275.
- [20] T. I. Karu, "Cellular and molecular mechanisms of photobiomodulation (low-power laser therapy)," *IEEE Journal of Selected Topics in Quantum Electronics*, vol. 20, no. 2, pp. 143–148, Mar. 2014, doi: 10.1109/JSTQE.2013.2273411.
- [21] H. Kohli, S. Srivastava, S. K. Sharma, S. Chouhan, and M. Oza, "Design of programmable LED based phototherapy system," *International Journal of Optics*, vol. 2019, pp. 1–8, Jun. 2019, doi: 10.1155/2019/6023646.
- [22] O. Chamorro-Atalaya, D. Goicochea-Vilela, D. Arce-Santillan, M. Diaz-Choque, and T. Diaz-Leyva, "Automation of the burner of a pilotubular boiler to improve the efficiency in the generation of steam," *Indonesian Journal of Electrical Engineering and Computer Science*, vol. 21, no. 1, pp. 101–109, 2021, doi: 10.11591/ijeecs.v21.i1.pp101-109.
- [23] R. Hassani, M. Boumechraz, and M. Hamzi, "Implementation of wheelchair controller using mouth and tongue gesture," *Indonesian Journal of Electrical Engineering and Computer Science*, vol. 24, no. 3, p. 1663, Dec. 2021, doi: 10.11591/ijeecs.v24.i3.pp1663-1671.
- [24] N. Watjanatepin, "Design and analysis of the PAR spectrum of the tunable red: Blue actual photon flux ratio of the LED lighting system," *Optoelectronics and Advanced Materials, Rapid Communications*, vol. 12, no. 11–12, pp. 652–659, 2018.
- [25] S. Zhang *et al.*, "Efficient emission of InGaN-based light-emitting diodes: toward orange and red," *Photonics Research*, vol. 8, no. 11, p. 1671, Nov. 2020, doi: 10.1364/PRJ.402555.
- [26] K. Liu, H. Chen, Y. Wang, M. Wang, and J. Tang, "Wearable flexible phototherapy device for knee osteoarthritis," *Electronics (Switzerland)*, vol. 10, no. 16, 2021, doi: 10.3390/electronics10161891.
- [27] R. H. Mahdi and H. A. Jawad, "Thermal response of skin diseased tissue treated by plasmonic nanoantenna," *International Journal of Electrical and Computer Engineering (IJECE)*, vol. 10, no. 3, p. 2969, 2020, doi: 10.11591/ijece.v10i3.pp2969-2977.
- [28] N. Watjanatepin, "Urban gardening system for home organic vegetables: LED artificial light and irrigation control," *Journal of Engineering and Technological Sciences*, vol. 52, no. 6, p. 805, Nov. 2020, doi: 10.5614/j.eng.technol.sci.2020.52.6.3.
- [29] N. Watjanatepin and P. Sritanauthaikorn, "Rectangular module for large scale solar simulator based on high-powered LEDs array," *Telkomnika (Telecommunication Computing Electronics and Control)*, vol. 20, no. 2, pp. 462–474, 2022, doi: 10.12928/TELKOMNIKA.v20i2.23308.

BIOGRAPHIES OF AUTHORS







Napat Watjanatepin     received the B.S. Tech. Ed. (Electrical Engineering) degree from Institute of Technology Vocational Education, Thailand in 1985, and M.S. Tech. Ed. (Electrical Technology) degree from King Mongkut's Institute of Technology North Bangkok, Thailand in 1991. His research interests include power electronics and drives, renewable energy, PV energy system, LED solar simulator, LED for horticulture and engineering educations. He can be contacted at email: napat.w@rmutsb.ac.th.



Paiboon Kiatsookkanatorn     received the B.S.Tech.Ed. and B.Eng. degrees from Rajamangala Institute of Technology, Thailand in 1998 and 2002, respectively, and the M.Eng. and Ph.D. degrees from Chulalongkorn University, Bangkok, Thailand in 2005 and 2012, respectively. He is currently an Assistant Professor in the Department of Electrical Engineering, Rajamangala University Suwanabhumi (RMUTSB), Thailand. His research interests include matrix converters and pulsewidth-modulation (PWM). He can be contacted at email: paiboon.k@rmutsb.ac.th.






Chaiyant Boonmee     received his B. Eng. in electrical engineering from Rajamangala Institute of Technology Thewes, his M. Eng degrees from Rajamangala University of Technology Thanyaburi and his Ph.D. degree in electrical engineering from Chiang Mai University (CMU), Chiang Mai, Thailand, in 2017. His research interests include power electronic application, multilevel cascaded inverters and IoT application. He can be contacted at email:chaiyant.b@rmutsb.ac.th.



Sarayoot Thongkullaphat    received the B.Ind. Tech. (Electrical Engineering) degree from South-East Asia University, Thailand in 1996, M. Eng. (Electrical Engineering) degree from King Mongkut's University of Technology Thonburi, Thailand in 2004, and Ph.D. (Electrical Engineering) degree from King Mongkut's University of Technology North Bangkok, Thailand in 2014. His research interests include power electronics and drives, control system, renewable energy, LED solar simulator, renewable energy. He can be contacted at email: sarayoot.t@rmutsb.ac.th.






Tuanjai Archevapanich    received the B.S. Tech.Ed. (Telecommunication Engineering) degree from King Mongkut's University of Technology Ladkrabang, Thailand in 1994. Her M. Eng degrees from Rajamangala University of Technology Thanyaburi and his D.Eng. (Electrical Engineering) degree from King Mongkut's University of Technology Ladkrabang, Thailand, in 2019. Her research interests include Electrical Measurements and Instrumentation, electronics device, and Engineering Education. She can be contacted at email: Tuanjai.a@rmutsb.ac.th.



Patcharanan Sritanauthaikorn    received the B. Eng. (Electrical Engineering) degree from Khon Kaen University, Thailand in 1998, and M. Eng. (Electrical Engineering) degree from King Mongkut's University of Technology Thonburi, Thailand in 2004. Her research interests include control system, automation, power electronics, renewable energy, LED solar simulator. She can be contacted at email: patcharanan.s@rmutsb.ac.th.



Khanittha Wannakam    received the B.S. in Electrical Engineering from Burapha University, Thailand, in 2007, and the M.S. degree in Electrical Engineering from Chulalongkorn University, Thailand, in 2010, and Ph.D. degree in Electrical Engineering from King Mongkut's Institute of Technology Ladkrabang, Bangkok, Thailand, in 2018. Her research interests are in power system reliability, neural networks in power systems, renewable energy, LED solar simulator, and LED for horticulture and engineering educations. She can be contacted at email: khanittha.w@rmutsb.ac.th.